6-22-2016

# MicroRNA miR-155 Is Necessary for Efficient Gammaherpesvirus Reactivation from Latency, but Not for Establishment of Latency

Rebecca L. Crepeau
*Dartmouth College*

Peisheng Zhang
*Dartmouth College*

Edward J. Usherwood
*Dartmouth College*

AMERICAN SOCIETY FOR MICROBIOLOGY | Journal of Virology

# MicroRNA miR-155 Is Necessary for Efficient Gammaherpesvirus Reactivation from Latency, but Not for Establishment of Latency

**Rebecca L. Crepeau, Peisheng Zhang, Edward J. Usherwood**

Department of Microbiology and Immunology, Geisel School of Medicine at Dartmouth, Lebanon, New Hampshire, USA

**ABSTRACT**

**MicroRNA-155 (miR-155) has been shown to play significant roles in the immune response, including in the formation of germinal centers (GC) and the development and maturation of T follicular helper (Tfh) cells. There is *in vitro* evidence to support a critical role for cellular miR-155 and viral miR-155 homologs in the establishment of gammaherpesvirus latency in B cells. We sought to determine the contribution of miR-155 to the establishment and maintenance of latency *in vivo* using murine gammaherpesvirus (MHV-68) infection. MHV-68-infected mice deficient in miR-155 exhibited decreases in GC B cells and Tfh cells. However, the frequencies of spleen cells harboring latent MHV-68 genomes were the same in both miR-155-deficient and wild-type (WT) mice. Similar latent loads were also observed in mixed bone marrow chimeric mice, where B cell-extrinsic effects of miR-155 deficiency were normalized. Interestingly, we observed markedly lower efficiency of reactivation from latency in miR-155-deficient cells, indicating an important role for miR-155 in this process. These *in vivo* data complement previous *in vitro* studies and lead to the conclusion that miR-155 is not necessary for the establishment or maintenance of gammaherpesvirus latency but that it does affect reactivation efficiency.**

**IMPORTANCE**

**Gammaherpesvirus infection leads to severe disease in immunosuppressed populations. miR-155 has been shown to play important roles in many pathological processes, including tumorigenesis and diseases caused by an overly aggressive immune response. Our work provides valuable *in vivo* data showing that miR-155 is dispensable for gammaherpesvirus latency but that it is critical for reactivation from latency, which is a crucial step in the viral life cycle.**

The herpesvirus family is a large and widely distributed family of double-stranded, enveloped DNA viruses. Their anatomical sites of latency and frequency of reactivation vary, resulting in a range of clinical manifestations. A defining feature of this virus family is the ability to establish latent infection within host cells. The gammaherpesviruses distinguish themselves by being lymphotropic, in most cases establishing latency in B cells, where coordinated programs of viral and host gene expression promote B cell differentiation to favor virus latency.

Gammaherpesviruses are of clinical interest due to the two human members of this viral subfamily: Epstein-Barr virus (EBV; human herpesvirus 4 [HHV-4]) and Kaposi's sarcoma-associated herpesvirus (KSHV; HHV-8). These viruses are closely associated with the development of malignancies in immunosuppressed populations. EBV was initially recovered from an endemic form of Burkitt's lymphoma, and it has been shown to hijack the B cell differentiation pathway in order to gain access into the long-lived memory B cell compartment (1). Due to the narrow host tropism and seroprevalence of the human gammaherpesviruses, murine gammaherpesvirus (MHV-68) has become a critical model system in which to examine the *in vivo* immunobiology of the gammaherpesviruses. Like its human counterparts, MHV-68 is a lymphotropic, double-stranded DNA virus that establishes latency in B cells (2, 3), primarily in the spleen.

Herpesviruses establish latent infection within host cells in order to persist for the lifetime of the host. Viral gene expression must be silenced in this state to avoid immune recognition; the virus must also modulate host cell functions, such as cellular life span, proliferation, and differentiation, in order to promote the latent state. To evade the immune response, the timing and amount of virus replication must be controlled. One of the ways in which this can occur is through the carefully choreographed expression of viral genes through posttranscriptional regulation via microRNAs (miRNAs).

By their ability to regulate large groups of genes simultaneously, miRNAs are attractive targets for viral manipulation to alter host cell processes. This class of small RNAs consists of regulatory, noncoding RNAs that bind to their mRNA targets and either block their translation or initiate their degradation. They do so through imperfect complementary base pairing in the 3′ untranslated region (UTR) (4). miRNAs have been shown to play important roles in various cellular and pathogenic processes, including cellular development and maturation, various immunological responses, and tumorigenesis (5–7).

The gammaherpesviruses encode multiple miRNAs which may mimic cellular miRNAs and modulate both cellular and viral gene expression as well as cellular miRNA expression. One microRNA in particular, miR-155, has been shown to control a wide range of immunological functions including T and B cell

**Received** 25 March 2016 **Accepted** 14 June 2016

**Accepted manuscript posted online** 22 June 2016

**Citation** Crepeau RL, Zhang P, Usherwood EJ. 2016. MicroRNA miR-155 is necessary for efficient gammaherpesvirus reactivation from latency, but not for establishment of latency. J Virol 90:7811–7821. doi:10.1128/JVI.00521-16.

**Editor:** R. M. Longnecker, Northwestern University

Address correspondence to Edward J. Usherwood, Edward.J.Usherwood@dartmouth.edu.

activation, inflammation, and immunological memory (8). Interestingly, KSHV and also the alphaherpesvirus Marek's disease virus encode viral homologs for cellular miR-155, indicating its likely role in herpesvirus pathogenesis. The KSHV homolog, miR-K12-11, as well as the Marek's disease virus homolog, mdv1-miR-M4, share 100% seed sequence specificity with human miR-155 and also have been shown to regulate a common set of target genes (9–11).

Mature miR-155 is derived from the B cell integration cluster (BIC)-associated noncoding RNA precursor (12). This gene was originally identified as a common retroviral insertion site for avian leukosis virus-induced B cell lymphomas (13). Despite the fact that EBV does not encode a viral homolog to miR-155, both the precursor *BIC* and, subsequently, the mature miR-155 transcripts have been shown to be overexpressed in EBV-infected cells as well as in a variety of EBV-associated B cell malignancies, indicating viral regulation of this cellular microRNA (14–16). Additionally, this overexpression was found to be induced by viral genes (14). When miR-155 was selectively inhibited in EBV-positive tumor cell lines *in vitro*, these cells failed to proliferate and underwent a higher rate of apoptosis, indicating a role for this microRNA in driving immortalization (17).

While previous studies have suggested an important role for miR-155 in the promotion of gammaherpesvirus latency, these studies largely relied on *in vitro* experiments. In this report we use MHV-68 infection to test whether the absence of cellular miR-155 in B cells affects latent infection *in vivo*. We find that both latency establishment and maintenance occur comparably in the absence of miR-155. However, in this setting, reactivation from latency occurs with lower efficiency, suggesting an important role for this miRNA in reemergence of the virus from the latent state. To date, few host factors have been found to influence latency and reactivation. This study provides evidence that host cellular miR-155 plays a critical role in reactivation from latency, a crucial step in the viral life cycle.

## MATERIALS AND METHODS

**Mice and virus.** C57BL/6 (B6) and B6-Ly5.2 mice were purchased from the National Cancer Institute (Bethesda, MD). The B6.Cg-Mir155$^{tm1.1Rsky}$/J strain (denoted miR-155 KO, where KO is knockout) was purchased from The Jackson Laboratories (Bar Harbor, ME) and bred in the Dartmouth-Hitchcock Medical Center animal facility. Mice were maintained under specific-pathogen-free conditions in the Dartmouth Center for Comparative Medicine and Research. The Animal Care and Use Committee of Dartmouth College approved all animal experiments.

MHV-68 clone G2.4 was obtained from A. A. Nash (University of Edinburgh, Edinburgh, United Kingdom). The viral strains were propagated, and titers were determined using NIH 3T3 cells, as previously described (18). A transgenic strain of MHV-68 harboring a fusion protein composed of the enhanced yellow fluorescent protein (EYFP) coding sequence fused to the histone H2b open reading frame, MHV-68–H2bYFP, was also used in order to determine the population of latently infected B cells. This strain was kindly provided by Samuel Speck (Emory University, Atlanta, GA). Mice were infected intranasally with 4,000 PFU MHV-68 or MHV-68–H2bYFP under anesthesia with isoflurane.

**Generation of mixed BM chimeric mice.** B6-Ly5.2 recipient mice were lethally irradiated with 1,000 rads (500 rads twice, given 24 h apart) and subsequently injected intravenously (i.v.) with a total of $1 \times 10^6$ to $2 \times 10^6$ bone marrow (BM) cells containing a mixture of B6-Ly5.2 (CD45.1$^+$) and miR-155 KO (CD45.2$^+$) cells at a 1:1 ratio. Reconstitution of the BM was checked at 5 weeks post-BM transfer by staining blood cells for the congenic markers.

**Tissue and cell preparations.** Splenocytes were prepared by passing spleens through cell strainers, and red blood cells (RBCs) were lysed using Gey's solution.

**Plaque assay.** Infectious virus titers in the lungs were determined by plaque assays as previously described (18). Briefly, lungs were homogenized and frozen at −80°C at 7, 8.5, or 10 days postinfection (dpi). Serial dilutions of homogenized lung tissues were added to NIH 3T3 monolayers in a minimal volume and left to adsorb for 1 h before samples were overlaid with carboxymethyl cellulose. After 5 days of incubation at 37°C, the assays were fixed with methanol and stained with Giemsa stain, and plaques were enumerated microscopically.

**Virus neutralization assay.** Blood was collected from mice latently infected with MHV-68 at 28 days postinfection. Six 3-fold dilutions of serum were made in duplicate, starting at a 1/10 dilution. The diluted serum samples were mixed with 50 PFU of MHV-68 and incubated at room temperature for 1 h. One hundred microliters of the mixture plus 400 μl of complete medium was then added to NIH 3T3 monolayers, which were then incubated at 37°C for 1 h. Two milliliters of medium containing carboxymethyl cellulose was then added, and the plates were cultured for 5 days at 37°C. On the sixth day, monolayers were fixed with methanol for 1 h and stained with Giemsa stain, and plaques were counted microscopically. The percentage of neutralization was calculated based on the maximum number of plaques in the no-serum control.

**β-Gal/LacZ assay.** For detection of β-galactosidase (β-Gal) activity, cells were stained with the β-galactosidase substrate resorufin β-D-galactopyranoside (RDG; Marker Gene, Inc., Eugene, OR). Briefly, splenocytes were harvested at 14 days postinfection and processed into a single-cell suspension of $2 \times 10^7$ cells/ml. One hundred microliters of prewarmed cell samples was loaded with 100 μl of 2 mM prewarmed RDG at 37° for 1 min. The reaction was stopped by mixing loaded samples with 2 ml of ice-cold Hanks balanced salt solution (HBSS) containing 2% serum, 10 mM HEPES, and 1% penicillin-streptomycin (HBSS+). Loaded cell samples were kept on ice for 1.5 h to allow accumulation of fluorochrome release from RDG in LacZ$^+$ cells. Samples were then pelleted and resuspended in 100 μl of ice-cold HBSS+. Samples were then stained with antibody markers of germinal center (GC) B cells as stated above and analyzed using the MACSQuant instrument in the DartLab core facility (Dartmouth College) or an Accuri flow cytometer. Data were analyzed using FlowJo software (TreeStar, Ashland, OR) or Accuri software (BD Biosciences).

**Abs and flow cytometry.** Antibodies (Abs) for flow cytometric analysis were purchased from eBioscience (San Diego, CA), BD Biosciences (San Jose, CA), or Biolegend (San Diego, CA). In germinal center B cells the following were used: T and B cell activation marker conjugated to phycoerythrin (GL7), CD19 conjugated to peridinin-chlorophyll protein-Cy5.5 (ID3), and CD95 conjugated to allophycocyanin (APC) (15A7). In plasma cells, the following were used: CD138 conjugated to phycoerythrin (281-2), CD3 conjugated to peridinin-chlorophyll protein-Cy5.5 (145-2C11), and B220 conjugated to Pacific blue (RA-3-6B2). In T follicular helper cells, the following were used: CD4 conjugated to allophycocyanin-eFluor 780 (GK1.5), purified CXCR5 (2G8), PD-1 conjugated to fluorescein isothiocyanate (FITC) (J43), BCL-6 conjugated to peridinin-chlorophyll protein-Cy5.5 (K112-91), biotin-conjugated Affinipure goat anti-rat IgG(H+L) (Jackson ImmunoResearch), and streptavidin-APC. Samples were analyzed using the MACSQuant instrument in the DartLab core facility (Dartmouth College) or Accuri flow cytometer. Data were analyzed using FlowJo software (TreeStar, Ashland, OR) or Accuri software (BD Biosciences).

Surface markers on cells were stained with Abs in phosphate-buffered saline (PBS) with 2% bovine growth serum ([BGS]; fluorescence-assisted cell sorting [FACS] buffer) at 4°C for 20 min. Tfh cells were stained with purified CXCR5 for 1 h in PBS plus 0.5% bovine serum albumin (BSA) plus 2% normal mouse serum (NMS) plus 2% BGS, followed by biotin-goat anti-rat IgG for 30 min in FACS buffer plus 2% NMS plus 2% BGS and then by streptavidin and additional surface-staining Abs for 30 min in

FACS buffer plus 2% NMS plus 2% BGS at 4°C. A Foxp3/transcription factor staining buffer set (eBioscience) was used for transcription factor detection.

**Quantitative PCR (qPCR) for viral load.** Latent viral DNA was quantified by quantitative fluorescent PCR (QF-PCR) as previously described (19). Briefly, DNA was extracted from whole splenocytes or sorted B cells using a Qiagen DNeasy kit (Qiagen, Valencia, CA) and then quantified using a UV spectrophotometer. DNA (300 ng) was subjected to QF-PCR using Platinum Quantitative PCR SuperMix-UDG (Invitrogen, Carlsbad, CA), 500 nM primers complementary to the *ORF50* gene, and 200 nM labeled probe complementary to the *ORF50* gene. The samples were subjected to 40 cycles of 15 s at 95°C and 1 min at 60°C. QF-PCR was performed using a Bio-Rad iCycler (Bio-Rad, Hercules, CA). To construct a standard curve, a graded number of copies of the pTW-27 plasmid, containing the genomic *ORF50* gene, was mixed with 300 ng of normal splenocyte DNA and subjected to QF-PCR. No-template controls containing 300 ng of uninfected splenocyte DNA were negative for all QF-PCR assays. The assay was able to detect fewer than 10 viral genomes per sample.

**Total serum IgG ELISA.** Blood was collected from mice latently infected with MHV-68 at 28 to 30 days postinfection. Serum samples were subjected to a mouse IgG total Ready-Set-Go enzyme-linked immunosorbent assay (ELISA) as instructed by the manufacturer (eBioscience, San Diego, CA). Briefly, Corning Costar 9018 ELISA plates (Corning, NY) were coated at 4° overnight with the provided capture antibody. The plate was washed, and wells were blocked for 2 h at room temperature with the provided blocking buffer. A standard curve was generated using 2-fold serial dilutions of the standard in 1× assay buffer A. Samples at a 1:1,000 dilution were added to the designated wells, followed by the provided detection antibody. The plate was covered and incubated at room temperature for 3 h, at which point substrate was added and allowed to incubate at room temperature. Reactions were stopped after 15 min and read at a wavelength of 450 nm.

**LDA measuring frequency of free or reactivatable virus.** Limiting-dilution assays (LDAs) were performed as described previously (20). Primary mouse embryonic fibroblasts (MEF) were added to flat-bottomed 96-well plates ($10^4$ cells/well) and cultured overnight. A spleen cell suspension was prepared using organs from infected mice, and graded numbers of cells (100,000 to 780 cells/well) were added to the MEF monolayers. Twenty-four replicate wells were used per dilution of spleen cells. The plates were cultured for 2 weeks at 37°C and then examined microscopically to determine the proportion of wells exhibiting cytopathic effect (CPE). A duplicate sample was subjected to a freeze-thaw, and then dilutions of this sample (100,000 to 12,000 cell equivalents/well) were cultured on MEF monolayers as described above to measure the level of cell-associated preformed virus. To calculate the frequency of cells reactivating from latency, the $\log_{10}$ percentage of wells with no CPE was plotted against the number of cells per well. The Poisson distribution predicts that if an average of one cell per well is latently infected, then 37% of wells will have no CPE. Thus, the frequency of latently infected cells was read from the number of cells per well, giving 37% of wells with no CPE. The frequency of preformed virus was $<1$ per $10^5$ cell equivalents in most cases and never greater than 1 per $4.6 \times 10^4$ cell equivalents.

**Determination of the frequency of latently infected cells by limiting-dilution PCR (LDA-PCR) analysis.** To determine the frequency of cells carrying the MHV-68 genome, nested PCR assays for MHV-68 gene 50 were performed on serial dilutions of cells by using a previously published method, with slight modifications (21). Briefly, test cells were thawed, washed, resuspended in an isotonic solution, and counted. Starting at $10^4$ cells/reaction mixture, cells were serially diluted 3-fold in a background of uninfected NIH 3T3 cells such that a total of $10^4$ cells were present in each well (10-μl total volume) and plated in a 96-well PCR plate at 12 wells/sample per experiment. Single copies of a plasmid containing MHV-68 gene 50 in a background of 3T3 cells were included as positive controls to verify sensitivity. 3T3 samples with no plasmid were included as negative controls. After overnight lysis of cells with proteinase K, round-one PCR was performed in 20 μl/reaction. A nested PCR (30 cycles) was performed following addition of 10 μl of round-two reaction buffer to the same well, and nested products were visualized on a 2% agarose gel.

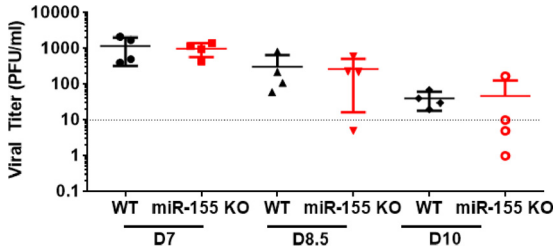


**FIG 1** miR-155 is not required for MHV-68 replication. WT C57BL/6 ($n = 4$) or miR-55 KO ($n = 4$) mice were infected with WT MHV-68 intranasally. Lungs were harvested at 7, 8.5, or 10 dpi (D7, D8.5, or D10, respectively), and lung homogenates were subjected to a standard plaque assay to determine viral titers. The dotted line indicates the threshold of detection. Data are representative of two independent experiments. Bars show standard deviations.

**Statistical analysis.** Statistical differences were determined using Student *t* tests or two-way analysis of variance (ANOVA) using GraphPad Prism, version 6, software (GraphPad, La Jolla, CA).

## RESULTS

**miR-155 is not required for MHV-68 replication.** To evaluate the role of miR-155 in MHV-68 replication, we infected wild-type (WT) C57BL/6 mice alongside miR-155 knockout (KO) mice with WT MHV-68 intranasally. Viral lung titers were determined at 7, 8.5, and 10 dpi by standard plaque assay. Titers in the lungs of both groups were similar at all time points tested, declining toward the limit of detection by 10 dpi (Fig. 1). These data indicate that miR-155 is dispensable for acute viral replication and control of MHV-68 replication *in vivo*.

**MHV-68 infection induces *BIC* expression in germinal center B cells.** miR-155 expression has been shown to be upregulated in both activated T and B cells as well as in EBV-transformed cell lines and clinically isolated B cell lymphoma samples (22–25). We first asked whether there would be a similar induction of miR-155 expression in GC B cells, the target cell population, following primary MHV-68 infection. To address this question we utilized heterozygous *BIC*/miR-155 knockout *lacZ* reporter mice, which allowed for detection of the transcriptional activity of the *BIC* promoter, the transcriptional unit giving rise to mature miR-155 transcripts, while preserving one intact copy of the *BIC* gene (24, 26). Several studies have shown that *BIC* transcription is directly correlated with expression of the mature miR-155 transcript (14–16). Splenocytes were harvested at 14 days postinfection (dpi) and were incubated with the fluorescent β-galactosidase substrate resorufin β-D-galactopyranoside. In order to compare miR-155 expression levels in both MHV-68-infected and uninfected GC B cells in the same animal, we utilized a transgenic virus harboring an EYFP-H2b fusion protein to detect cells that were latently infected with MHV-68 (Fig. 2A) (27). Using this system we determined that *BIC*/miR-155 transcription was upregulated in MHV-68-infected GC B cells compared to levels in their uninfected counterparts (Fig. 2B and C).

**miR-155 deficiency leads to an aberrant GC response following MHV-68 infection.** miR-155 has been shown to play an important role in the generation of germinal center responses in Peyer's patches and after immunization with model antigens (26,

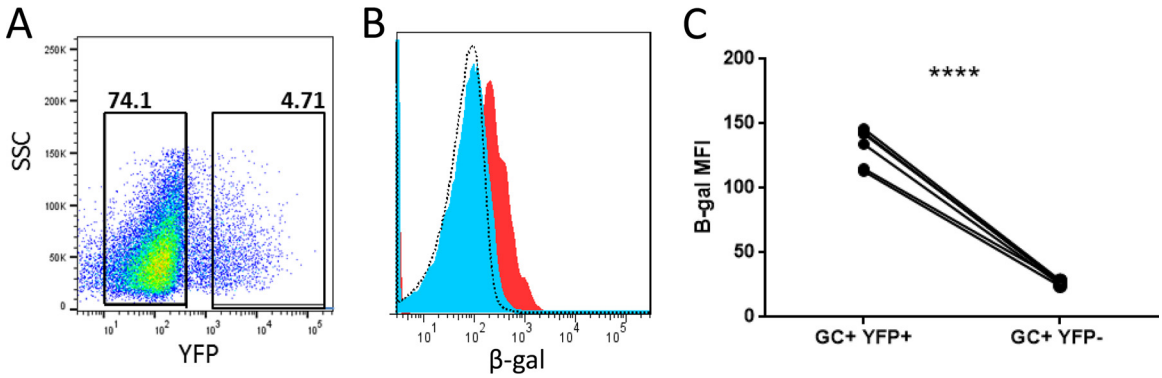


**FIG 2** miR-155 is upregulated in MHV-68-infected GC B cells. The miR-155 KO locus contains a β-galactosidase (LacZ) reporter gene in exon 2 of the *BIC* gene. miR-155-heterozygous mice ($n = 6$) were infected with an MHV-68-H2bYFP reporter virus intranasally. Splenocytes were harvested at 14 dpi. (A) Infected ($YFP^+$) and uninfected (YFP negative [$YFP^-$]) populations were determined from the GC B cell compartment ($CD19^+$ $GL7^+$ $CD95^+$) using flow cytometry. Numbers show the percentages of cells in the gates shown. SSC, side scatter. (B) Representative histogram of the mean fluorescence intensity (MFI) of β-Gal expression gated on infected (red) and uninfected (blue) GC B cells. The dotted peak represents the no-substrate control. (C) Quantification of β-Gal expression, with each pair of points representing samples from a single mouse. Plots are representative of two independent experiments. ****, $P < 0.0001$, as determined using Student's *t* test.

28). However, it is not clear whether this requirement is altered following viral infection and particularly in infections such as those with MHV-68 that drive a potent splenic germinal center response. To address this question, miR-155 KO and WT C57BL/6 mice were infected with WT MHV-68 intranasally. Spleens were harvested at 14 dpi and analyzed by flow cytometry using the phenotypic markers indicated in Fig. 3. The GC B cell population was measured by surface expression of GL7 and CD95 on $CD19^+$ B cells (Fig. 3A). Though total B cell numbers did not differ between groups (data not shown), the proportion and absolute numbers of GC B cells were found to be reduced significantly in the miR-155 KO animals (Fig. 3B and C).

It has become well established that T follicular helper (Tfh) cells are necessary for the development of a proper germinal center response and that this response in turn fuels the differentiation of more Tfh cells (29, 30). The Tfh cell response has been reported to be necessary for optimal latency establishment in MHV-68 infection (31); therefore, we tested whether miR-155 was necessary for this process. Tfh cell populations in mice can be readily detected using surface expression of CD4 and high expression of both CXCR5 and PD-1 (Fig. 3D). We detected a significant decrease in both the proportions and absolute numbers of these cells in our miR-155 KO animals compared to levels in WT C57BL/6 controls (Fig. 3E and F). These cells were confirmed to be Tfh cells by increased nuclear expression of the transcription factor BCL-6 and also by increased surface expression of the costimulatory molecule ICOS (Fig. 3G and H), increases which are consistent with their identity as Tfh cells (29, 32, 33). Interestingly, we also observed a statistically significant decrease in the level of ICOS expression in the miR-155 KO cells compared to the level in WT C57BL/6 cells (Fig. 3H). Taken together with the reduced germinal center response, these data confirm that miR-155 is required for an optimal germinal center reaction in the presence of the strong stimulation provided by gammaherpesvirus infection.

**miR-155 KO mice display a normal MHV-68-specific antibody response despite having fewer antibody-producing cells.** Because we observed a reduction in germinal center responses during MHV-68 infection, we next examined the frequency of plasma cell formation in the spleens of these mice. At 14 dpi there was a reduction in both the proportion and absolute number of $CD138^+$ plasma cells in the spleens of miR-155 KO animals compared to levels in WT C57BL/6 controls (Fig. 4A to C). Isotype-switched B cells are also associated with the development of, and transition through, the germinal center response. Therefore, we next measured the frequency of class-switched B cells using an antibody cocktail to determine surface expression of IgM, IgA, IgG1, or IgG2a. At 14 dpi there was a statistically significant decrease in the proportion of isotype-switched B cells in the spleens of miR-155 KO mice compared to levels in the WT C57BL/6 controls (Fig. 4D). Taken together with our GC observations, these data indicate that miR-155 is necessary for an optimal B cell response to MHV-68 infection.

The observed decrease in both the number of antibody producing cells and proportion of isotype-switched B cells in the miR-155 KO mice suggested that there would be a concomitant defect in antibody production. To address this, we tested whether the neutralizing antiviral antibody response was affected by miR-155 deficiency. We performed an *in vitro*, MHV-68-specific antibody neutralization assay, which measures the ability of serum antibody to neutralize MHV-68. We found that miR-155 KO animals were able to mount a neutralizing antibody response to MHV-68 that was comparable to that of WT mice even though they have fewer total antibody-producing cells (Fig. 4E), and this correlated with equivalent levels of total serum IgG levels in these mice (Fig. 4F).

**The requirement for miR-155 in the germinal center response is B cell intrinsic.** miR-155 knockout mice lack this miRNA in all cells; therefore, it is not possible to distinguish between cell-intrinsic effects and indirect effects due to miR-155 deficiency in other cell types. To address cell-intrinsic effects, we generated mixed-bone marrow (BM) chimeras using a 1:1 mixture of WT C57BL/6 and miR-155 KO BM injected into lethally irradiated, congenically distinct recipients. These mice possess both WT and miR-155-deficient T and B cell populations, distinguishable by congenic markers. As cells of both genotypes are present in the same animal, cell-extrinsic effects are controlled for, allowing measurement of the phenotype due to cell-intrinsic effects alone. Following engraftment at 5 weeks posttransplant, these animals exhibited similar proportions and numbers of B and

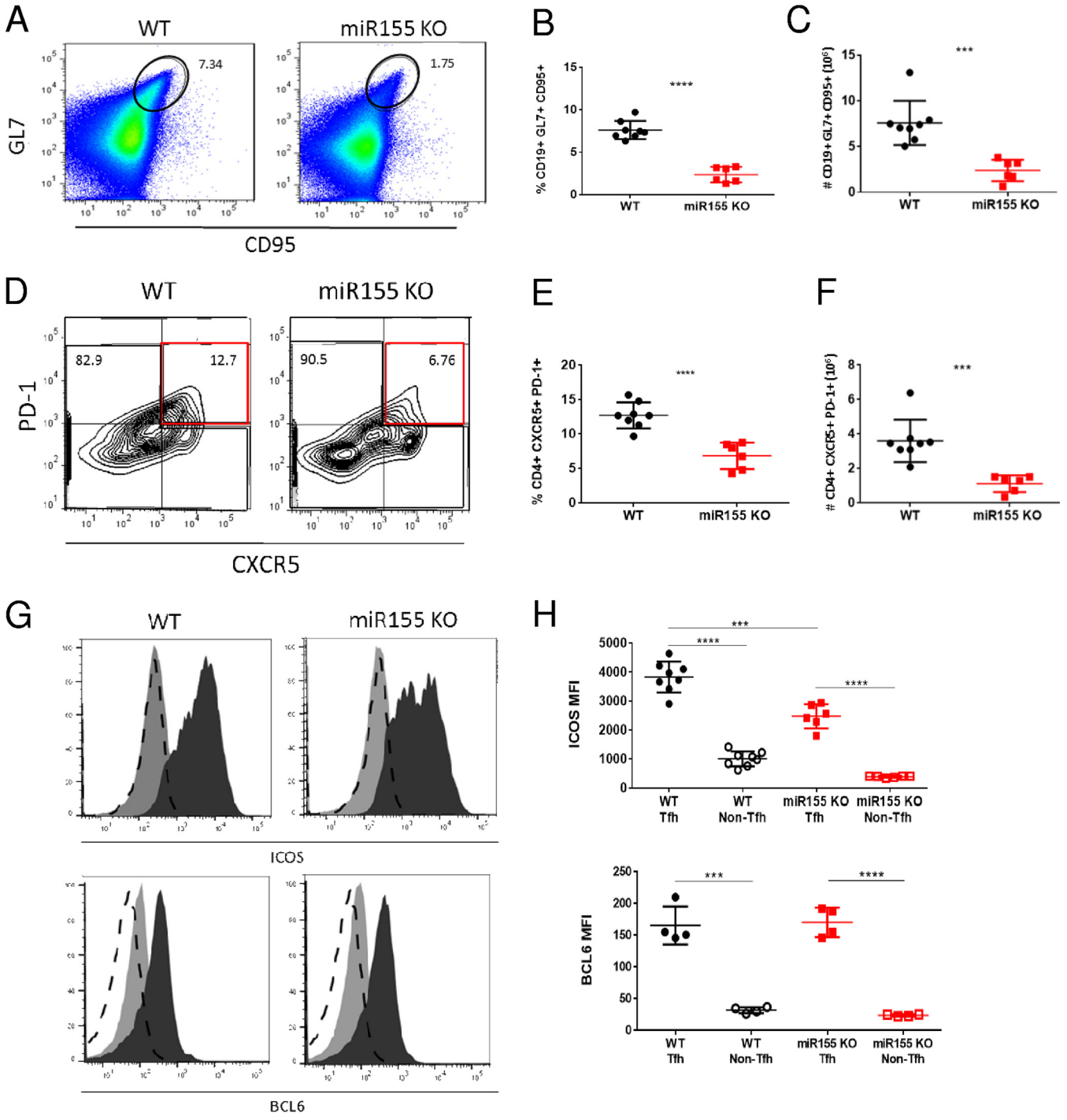


**FIG 3** miR-155 deficiency leads to an aberrant GC response following MHV-68 infection. WT C57BL/6 and miR-155 KO mice were infected with MHV-68 intranasally. Splenocytes were harvested at 14 dpi. (A) GC B cell ($GL7^+$ $CD95^+$) populations were measured using flow cytometry. Plots were gated on the $CD19^+$ population. (B) Percentages of GC B cells in WT C57BL/6 ($n = 8$) and miR-155 KO ($n = 6$) mice. (C) Absolute numbers of GC B cells within the total $CD19^+$ B cell population. (D) T follicular helper (Tfh) cell ($PD\text{-}1^+$ $CXCR5^+$) populations were measured using flow cytometry. Plots were gated on the $CD4^+$ population. (E) Percentages of Tfh cells in WT C57BL/6 ($n = 8$) and miR-155 KO ($n = 6$) mice. (F) Absolute numbers of Tfh cells within the $CD4^+$ T cell population. (G) Representative histograms of ICOS staining (top) and BCL-6 staining (bottom). Black peaks, Tfh cells; gray peaks, non-Tfh cells; dotted peaks, isotype. (H) Tfh cells express higher levels of ICOS (top) and BCL-6 (bottom) than non-Tfh cell populations. Each point represents data from an individual mouse. Data are representative of three independent experiments. MFI, mean fluorescence intensity. ***, $P < 0.001$; ****, $P < 0.0001$, as determined using Student's *t* test.

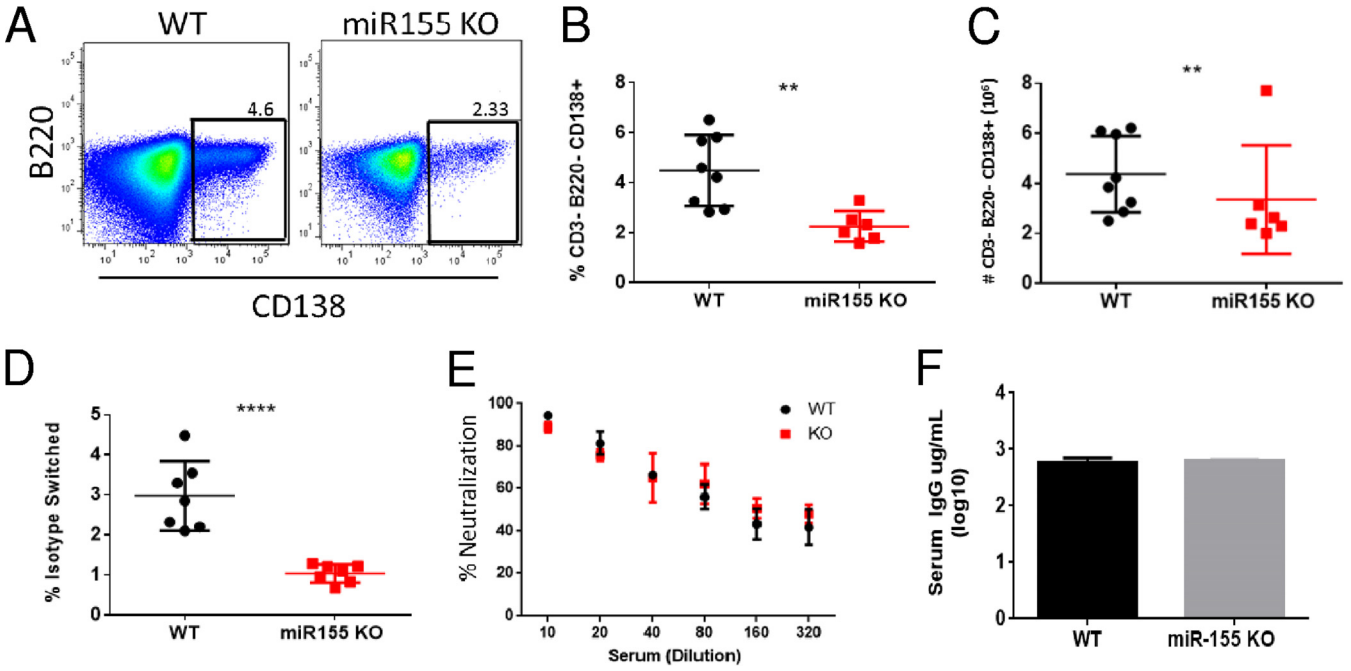


**FIG 4** miR-155 KO mice display a normal MHV-68-specific antibody response even though they have fewer antibody-producing cells. WT C57BL/6 and miR-155 KO mice were infected with MHV-68 intranasally. Splenocytes were harvested at 14 dpi. (A) Plasma cell ($B220^-$ $CD138^+$) populations in the spleen were measured using flow cytometry. Cells were gated on the $CD3^-$ $B220^-$ population. (B) Percentages of plasma cells in WT C57BL/6 ($n = 8$) and miR-155 KO ($n = 6$) mice. (C) Absolute numbers of plasma cells within the $CD3^-$ $B220^-$ population. (D) Percentages of isotype-switched ($IgM^+$/$IgG1^+$/$IgG2a^+$/$IgA^+$) B cells in WT C57BL/6 ($n = 7$) and miR-155 KO ($n = 7$) mice. Cells were gated on $CD19^+$ cells. (E and F) Serum samples from WT C57BL/6 ($n = 4$) and miR-155 KO ($n = 4$) mice were harvested at 28 dpi; their ability to neutralize MHV-68 was measured (E), and the total serum IgG levels were detected by ELISA (F). **, $P < 0.01$; ****, $P < 0.0001$, as determined using Student's *t* test.

T cells ($CD19^+$ and $CD3^+$, respectively) (data not shown). Following intranasal infection of these mixed chimeric animals with WT MHV-68, there again was a 2-fold decrease in both the proportion and absolute number of GC B cells at 14 dpi (Fig. 5A). As expected, this 2-fold decrease in the GC response led to a concomitant decrease in the proportion and number of plasma cells in the spleen at 14 dpi (Fig. 5B). Additionally, there was also a similar decrease in the proportion and number of Tfh cells in MHV-68-infected mixed chimeric animals (Fig. 5C), indicating a cell-intrinsic role for miR-155 for efficient Tfh cell responses. Taken together, these data indicate that miR-155 is required to form an optimal germinal center response during gammaherpesvirus infection and that this requirement is intrinsic to both B and Tfh cells.

**miR-155 is dispensable for the efficient establishment of latency in MHV-68 infection.** It is well recognized that the gammaherpesviruses preferentially attack the germinal center B cell compartment in order to establish latency and gain access to the long-lived memory B cell pool (2, 3). Since a decrease in germinal center B cells was seen in miR-155 KO mice compared with the level in WT C57BL/6 mice (Fig. 3), we examined whether this would have an effect on the establishment of latency in MHV-68 infection. To address this question we determined the frequency of cells harboring viral genome at the peak of latency (14 dpi) in miR-155-deficient and WT C57BL/6 mice, using a limiting-dilution PCR (LDA-PCR) approach as previously described (21). The data are plotted as the percentages of wells that contain viral genome (PCR positive). We found that the frequencies of cells harboring viral genome were similar between miR-155 KO animals (1 in 750 cells) and the WT C57BL/6 controls (1 in 500 cells) at the peak of latent infection (Fig. 6A). To confirm these data, we utilized a recombinant virus harboring an EYFP-H2b fusion protein which allowed us to measure the proportion of cells harboring latent virus on a per-cell basis (27). Within the GC B cell compartment ($CD19^+$ $GL7^+$ $CD95^+$) at 14 dpi, there was no difference in the proportions of YFP-positive ($YFP^+$) cells between the miR-155 KO animals and the WT C57BL/6 controls, indicating similarly sized populations of latently infected cells (Fig. 6B). The same was true when mixed chimeric animals were analyzed (Fig. 6C). Finally, when GC B cells were sorted from mixed chimeric animals and viral genome copy numbers were measured by quantitative PCR (qPCR) specific for MHV-68 *ORF50*, there was again no difference in the latent viral load between the miR-155 KO and WT C57BL/6 control animals (Fig. 6D). Interestingly, there was a statistically significant difference in viral DNA burdens in the non-GC population between WT and miR-155 KO animals; however, this represents a very small proportion of the total latent virus burden. These data also confirmed previous studies which documented that the majority of viral DNA resides in the GC B cell compartment rather than in other $CD19^+$ populations (2, 3).

**miR-155 is required for efficient reactivation from latency.** Given that miR-155 KO mice were able to establish latency at levels comparable to those of WT C57BL/6 mice, we next assessed the reactivation efficiency of cells from miR-155 KO mice using an *ex vivo* reactivation assay (21). This assay showed an approximate 50-fold decrease in the ability of miR-155 KO cells to reactivate from latency (1 in 50,000) compared to the ability in WT C57BL/6 control mice (1 in 1,000) (Fig. 7A). In contrast, the frequencies of

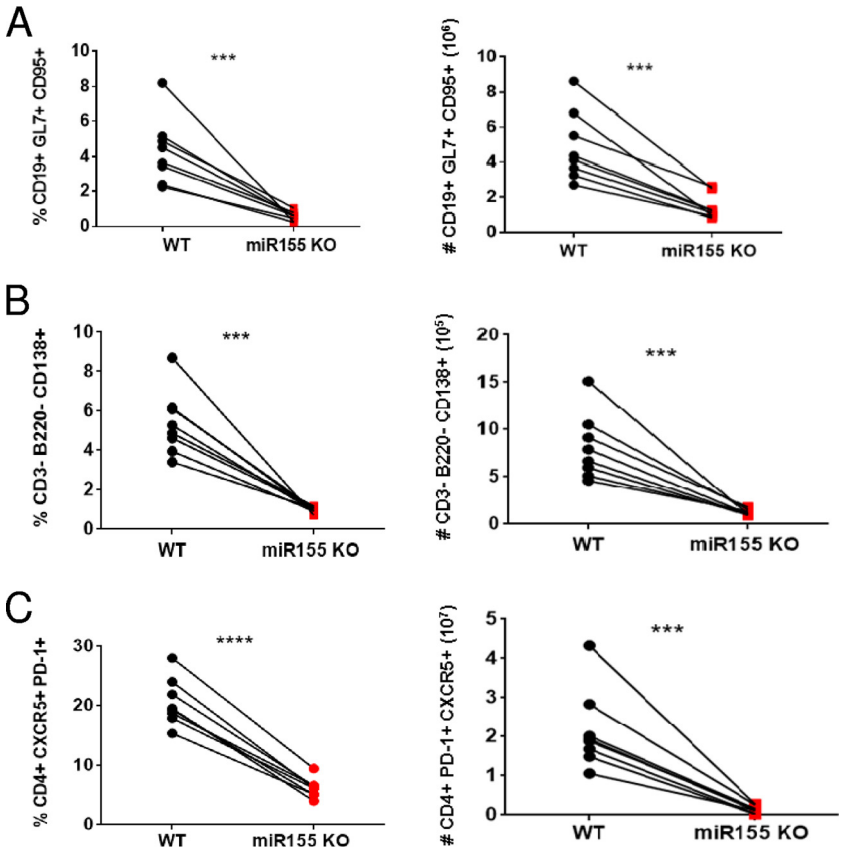


**FIG 5** The requirement for miR-155 in the GC response is B cell intrinsic. Mixed-bone marrow chimeric mice were infected with WT MHV-68 intranasally. Splenocytes were harvested at 14 dpi. Congenic markers were used to distinguish WT ($CD45.1^+$) from miR-155 KO ($CD45.2^+$) cells. Percentages (left) and absolute numbers (right) of GC B cells (A), plasma cells (B), and Tfh cells (C) are shown. Each point represents data from an individual mouse. Data are representative of three independent experiments. ***, $P < 0.001$; ****, $P < 0.0001$, as determined using Student's *t* test.

viral genome-bearing cells were not significantly different, as determined by LDA-PCR on samples from the same mice (1 in 400 for WT compared to 1 in 100 for miR-155 KO mice) (Fig. 7B). These data therefore indicate a significant defect in the reactivation efficiency of miR-155-deficient cells.

## DISCUSSION

The herpesviruses are unique in that they encode more microRNAs than most other virus families. The gammaherpesviruses are chief among these, encoding as many as 44 viral miRNAs (34, 35). Both virus-encoded and cellular miRNAs can alter the transcription of viral and cellular genes during infection. Of particular interest, KSHV encodes a viral homolog of the cellular miR-155 and has been shown to regulate a common set of target genes (9, 10). On the other hand, EBV does not encode a viral homolog but, instead, is able to induce expression of cellular miR-155, which has been shown to promote enhanced cell survival and immortalization (14, 17, 36). Thus, the human gammaherpesviruses use two different strategies to regulate miR-155 target genes.

Due to the narrow host tropism of the human gammaherpesviruses, all previous studies utilizing EBV infection were performed *in vitro* and only measured the effect of miR-155 inhibition after latent infection was established. Recent work has shown that gene expression profiling using *in vitro* cell lines does not always correlate with expression in the equivalent cells when they are infected *in vivo* (37). To date, there have been no studies addressing an *in vivo* role for miR-155 in infection or pathogenesis following gammaherpesvirus infection. The work discussed here sought to examine whether latency establishment is affected by the absence of miR-155 *in vivo*. MHV-68 has become a critical model system in which to study such *in vivo* questions. Here, we show that, like EBV, MHV-68 is able to induce *BIC* expression in latently infected cells. Additionally, although there is a cell-intrinsic role for miR-155 in the GC response following MHV-68 infection, it is dispensable for latency establishment. We also show a novel role for miR-155 in reactivation from latency, a crucial step in the viral life cycle.

Early work found that miR-155 deficiency led to both fewer and smaller germinal centers in the gut-associated lymphoid tissue of naive mice and in secondary lymphoid tissue following vaccination with model antigens, indicating its critical role in the germinal center response (26, 28). Our finding of a cell-intrinsic role for miR-155 in the GC response is consistent with these data, as well as with data from a more recent study following infection with attenuated *Salmonella*, which showed a B cell-intrinsic role for miR-155 in both the generation of long-lived plasma cells and in isotype switching and affinity maturation (38).

BCL-6 is a critical transcription factor for the development of the Tfh cell population (29, 32). Interestingly, despite the fact that we found BCL-6 to be expressed equivalently in WT and miR-155

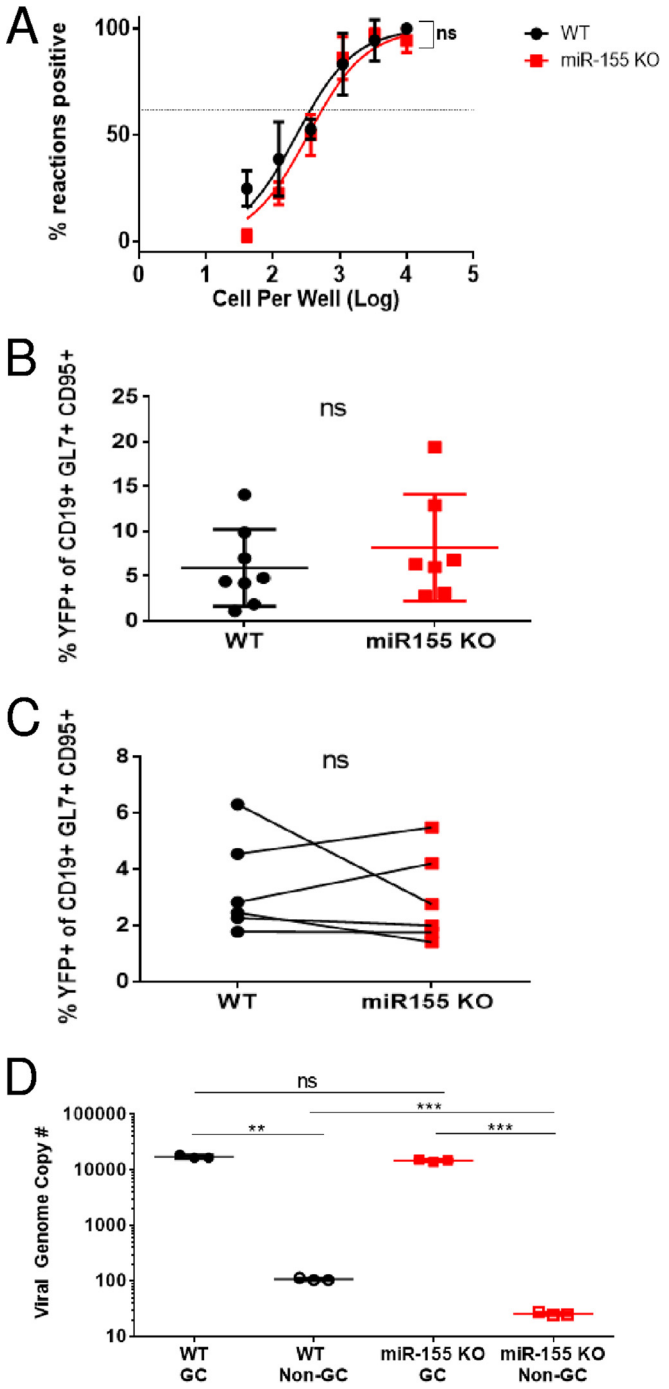


**FIG 6** miR-155 is dispensable for the efficient establishment of latency in MHV-68 infection. Mice were infected with WT MHV-68 or the MHV-68–H2bYFP reporter virus intranasally. Splenocytes were harvested at 14 dpi. (A) The frequency of cells harboring viral genome was determined using LDA-PCR. Flow cytometry was used to determine the proportion of cells harboring the viral genome from WT C57BL/6 ($n = 8$) or miR-155 KO ($n = 6$) mice (B) or mixed chimeric mice ($n = 6$) (C) infected with MHV-68–H2BYFP. (D) Mixed chimeric mice ($n = 6$) were infected with WT MHV-68, and spleens were pooled for sorting. DNA from sorted cell populations was subjected to qPCR analysis with primers specific to viral *ORF50*. Each point represents an individual mouse. Data represent two to three independent experiments. **, $P < 0.01$; ***, $P < 0.001$; ns, not significant (determined using Student's *t* test).

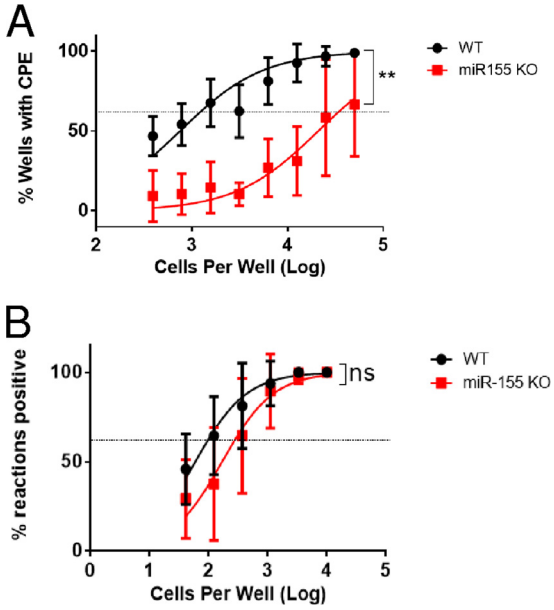


**FIG 7** miR-155 is required for efficient reactivation from latency. WT C57BL/6 ($n = 4$) or miR-155 KO ($n = 4$) mice were infected with WT MHV-68 intranasally. Splenocytes were harvested at 14 dpi for quantification of the frequency of cells reactivating virus (A) and the frequency of viral genome-positive cells (B) by LDA-PCR. Data are representative of two independent experiments. **, $P < 0.01$, as determined using Student's *t* test.

KO animals, we found a significant decrease in the proportion and number of Tfh cells in miR-155 KO mice. This is consistent with a recent study in a model of chronic inflammation showing regulation of Tfh cell numbers by miR-155 through both NF-κB and mTOR signaling (39). Since Tfh cells are needed to help drive the GC response, it is tempting to conclude that the deficiency in the GC response that we see in our miR-155 KO animals is due to the deficiency in the Tfh cell population. However, data generated from our chimeric animals showing cell-intrinsic roles for miR-155 in both the B cell and Tfh cell compartments negate this conclusion. Consistent with these data, previous studies showed that when miR-155 was deleted only within the T cell population, no deficit in the number of GC B cells was seen following ovalbumin (OVA) immunization (39). Interestingly, we also observed a significant decrease in surface ICOS expression on the Tfh cells from miR-155 KO mice. ICOS deficiency has been shown not only to cause a severe reduction in the number of T helper cells within the GC but also to mimic severe immunodeficiencies in humans (40, 41).

Several studies have shown that EBV induces miR-155 expression through induction of its host gene, *BIC*, following infection and that this upregulation is induced by viral genes (14, 15, 42, 43). Here, we show that MHV-68 is also able to induce *BIC*/miR-155 expression in infected GC B cells following infection, implying that this molecule may play a role in viral pathogenesis. We found no difference in viral lung titers at 7 dpi when miR-155 was absent, indicating that this molecule is not necessary for acute viral replication in the lung. This is in contrast to *in vitro* data from EBV and other viral systems, where miRNAs have been shown to play an inhibitory role in viral replication (44–47).

High expression of miR-155 in latently infected cells and in EBV-associated tumors suggests that miR-155 plays an important

role in maintaining latency. However, it has been shown that the different stages of latency seen in EBV infection are associated with differing levels of miR-155 expression. During the first few weeks of infection, EBV initiates a growth program, termed latency III, which includes all nine latency-associated genes. These genes provide proliferation, migration, and survival signals for the activated B cells. During this growth stage, miR-155 was found to be highly expressed. However, following the growth phase, when infected cells exhibit the latency I phenotype and only one of the nine proteins is still expressed (EBNA-1), miR-155 expression is downregulated, resulting in very low levels of both *BIC* transcription and of mature miR-155 transcripts (42, 48). Early (14 dpi) latency in the MHV-68 model is believed to be analogous to latency III of EBV, with a relatively broad expression of latency-associated genes. Therefore, our observations of elevated *BIC*/miR-155 expression at this time point are consistent with miR-155 upregulation in EBV latency III. Due to the low frequencies of latently infected cells at later times postinfection and to technical limitations in directly identifying latently infected cells at these late time points, we are currently unable to determine whether *BIC*/miR-155 is downregulated in long-term latently infected cells.

In this study, we report a 2-fold deficit in the target GC B cell population in miR-155 KO animals. However, we were surprised to find that when this decrease is taken into account, there was no significant reduction in the proportion of latently infected cells, indicating that miR-155 is dispensable for latency establishment. This was an interesting *in vivo* finding because both induced cellular miR-155 and the virally encoded orthologue have been shown to indirectly facilitate human gammaherpesvirus persistence *in vitro*. They are thought to act through targeting genes responsible for the expansion of the target cell population (17, 43, 49–51) and for inhibiting apoptosis through the regulation of viral genes (52, 53). This observation raises the important question of whether miR-155 is necessary for *in vivo* B cell latency in EBV and KSHV infection. Several other miRNAs have also been reported to influence latent gammaherpesvirus infection. For example, in EBV, multiple viral miRNAs have been found to be important in the survival of latently infected cells (54–56). The same is true for KSHV (57–59). Additionally, a recent study found that deletion of all 14 MHV-68-encoded miRNAs led to attenuated latency establishment (37), indicating that other viral miRNAs are able to promote latency establishment in several gammaherpesvirus infections.

Viral miRNAs have also been shown to be important for gammaherpesvirus reactivation from latency, typically by playing inhibitory roles. This is mediated either by direct repression of Rta or Zta, viral transcription factors that initiate lytic cycle replication, or indirectly through repression of the pathways leading to transcription of these factors (60–64). The KSHV homolog of miR-155, miR-K12-11, specifically was shown to inhibit Rta by inhibiting transcription factors known to activate the Rta promoter (64).

In contrast, the role of cellular miRNAs is more complex. Some inhibit reactivation through targeting of Rta or other EBV reactivation genes (65, 66). However, others have been found to enhance reactivation through the suppression of ZEB1 and ZEB2, which have been shown to bind to an inhibitory element in the Zta promoter (67, 68). Our finding that the lack of cellular miR-155 reduces MHV-68 reactivation efficiency may involve a mechanism similar to that of the latter case, which will be a focus of future studies.

Another aspect of gammaherpesvirus reactivation that has been well documented is the role that B cell maturation and differentiation play in this process (69, 70). Plasma cell differentiation was linked to virus reactivation in human gammaherpesvirus infection through the induction of the plasma cell transcription factor, XBP-1, which was found to induce a lytic switch and result in viral reactivation (71, 72). In MHV-68 infection XBP-1 was found to transactivate Rta *in vitro*; however, it was dispensable for reactivation after *in vivo* infection. In contrast, IRF4 was found to be essential for reactivation *in vivo* following MHV-68 infection due to its requirement in the generation of plasma cells (73). In this study, we found a cell-intrinsic defect in plasma cell differentiation in the miR-155 KO mice, which led to a 2-fold difference in the proportion and absolute number of plasma cells compared to the levels in the WT controls. This is consistent with previous studies (38, 74). However, this defect alone cannot explain the roughly 50-fold difference we found in reactivation efficiency between the miR-155 KO mice and the WT controls. miR-155 must therefore play a role in promoting reactivation, presumably by regulating key cellular and/or viral genes associated with this process. Future studies will be necessary to identify key miR-155 target genes that affect MHV-68 reactivation.

In conclusion, miR-155 has been shown to be important in promoting latency in human gammaherpesvirus infection; however, the previous studies were done primarily *in vitro*. Here, we present *in vivo* data showing that although miR-155 is dispensable for latent infection, it plays an important role in viral reactivation.

## FUNDING INFORMATION

This work, including the efforts of Edward J. Usherwood, was funded by HHS | National Institutes of Health (NIH) (R01CA103642). This work was funded by HHS | National Institutes of Health (NIH) (T32AI007363).

## REFERENCES

1. **Roughan JE, Thorley-Lawson DA.** 2009. The intersection of Epstein-Barr virus with the germinal center. J Virol **83:**3968–3976. http://dx.doi.org/10.1128/JVI.02609-08.
2. **Willer DO, Speck SH.** 2003. Long-term latent murine gammaherpesvirus 68 infection is preferentially found within the surface immunoglobulin D-negative subset of splenic B cells in vivo. J Virol **77:**8310–8321. http://dx.doi.org/10.1128/JVI.77.15.8310-8321.2003.
3. **Flaño E, Kim I-J, Woodland DL, Blackman MA.** 2002. γ-Herpesvirus latency is preferentially maintained in splenic germinal center and memory B cells. J Exp Med **196:**1363–1372. http://dx.doi.org/10.1084/jem.20020890.
4. **Bartel DP.** 2004. MicroRNAs: genomics, biogenesis, mechanism, and function. Cell **116:**281–297. http://dx.doi.org/10.1016/S0092-8674(04)00045-5.
5. **Chen C-Z, Li L, Lodish HF, Bartel DP.** 2004. MicroRNAs modulate hematopoietic lineage differentiation. Science **303:**83–86. http://dx.doi.org/10.1126/science.1091903.
6. **Di Leva G, Garofalo M, Croce CM.** 2014. MicroRNAs in cancer. Annu Rev Pathol **9:**287–314. http://dx.doi.org/10.1146/annurev-pathol-012513-104715.
7. **Lindsay MA.** 2008. MicroRNAs and the immune response. Trends Immunol **29:**343–351. http://dx.doi.org/10.1016/j.it.2008.04.004.
8. **Vigorito E, Kohlhaas S, Lu D, Leyland R.** 2013. miR-155: an ancient regulator of the immune system. Immunol Rev **253:**146–157. http://dx.doi.org/10.1111/imr.12057.
9. **Skalsky RL, Samols MA, Plaisance KB, Boss IW, Riva A, Lopez MC, Baker HV, Renne R.** 2007. Kaposi's sarcoma-associated herpesvirus encodes an ortholog of miR-155. J Virol **81:**12836–12845. http://dx.doi.org/10.1128/JVI.01804-07.
10. **Gottwein E, Mukherjee N, Sachse C, Frenzel C, Majoros WH, Chi J-TA, Braich R, Manoharan M, Soutschek J, Ohler U, Cullen BR.** 2007. A viral

microRNA functions as an ortholog of cellular miR-155. Nature **450:** 1096–1099. http://dx.doi.org/10.1038/nature05992.

11. **Morgan R, Anderson A, Bernberg E, Kamboj S, Huang E, Lagasse G, Isaacs G, Parcells M, Meyers BC, Green PJ, Burnside J.** 2008. Sequence conservation and differential expression of Marek's disease virus microRNAs. J Virol **82:**12213–12220. http://dx.doi.org/10.1128/JVI.01722-08.
12. **Tam W.** 2001. Identification and characterization of human BIC, a gene on chromosome 21 that encodes a noncoding RNA. Gene **274:**157–167. http://dx.doi.org/10.1016/S0378-1119(01)00612-6.
13. **Tam W, Ben-Yehuda D, Hayward WS.** 1997. *bic*, a novel gene activated by proviral insertions in avian leukosis virus-induced lymphomas, is likely to function through its noncoding RNA. Mol Cell Biol **17:**1490–1502. http://dx.doi.org/10.1128/MCB.17.3.1490.
14. **Rahadiani N, Takakuwa T, Tresnasari K, Morii E, Aozasa K.** 2008. Latent membrane protein-1 of Epstein-Barr virus induces the expression of B-cell integration cluster, a precursor form of microRNA-155, in B lymphoma cell lines. Biochem Biophys Res Commun **377:**579–583. http://dx.doi.org/10.1016/j.bbrc.2008.10.007.
15. **Yin Q, McBride J, Fewell C, Lacey M, Wang X, Lin Z, Cameron J, Flemington EK.** 2008. MicroRNA-155 is an Epstein-Barr virus-induced gene that modulates Epstein-Barr virus-regulated gene expression pathways. J Virol **82:**5295–5306. http://dx.doi.org/10.1128/JVI.02380-07.
16. **Kluiver J, Poppema S, de Jong D, Blokzijl T, Harms G, Jacobs S, Kroesen B-J, van den Berg A.** 2005. BIC and miR-155 are highly expressed in Hodgkin, primary mediastinal and diffuse large B cell lymphomas. J Pathol **207:**243–249. http://dx.doi.org/10.1002/path.1825.
17. **Linnstaedt SD, Gottwein E, Skalsky RL, Luftig MA, Cullen BR.** 2010. Virally induced cellular microRNA miR-155 plays a key role in B-cell immortalization by Epstein-Barr virus. J Virol **84:**11670–11678. http://dx.doi.org/10.1128/JVI.01248-10.
18. **Sunil-Chandra NP, Efstathiou S, Arno J, Nash AA.** 1992. Virological and pathological features of mice infected with murine gamma-herpesvirus 68. J Gen Virol **73:**2347–2356. http://dx.doi.org/10.1099/0022-1317-73-9-2347.
19. **Usherwood EJ, Ward KA, Blackman MA, Stewart JP, Woodland DL.** 2001. Latent antigen vaccination in a model gammaherpesvirus infection. J Virol **75:**8283–8288. http://dx.doi.org/10.1128/JVI.75.17.8283-8288.2001.
20. **Weck KE, Barkon ML, Yoo LI, Speck SH, Virgin HW IV.** 1996. Mature B cells are required for acute splenic infection, but not for establishment of latency, by murine gammaherpesvirus 68. J Virol **70:**6775–6780.
21. **Weck KE, Kim SS, Virgin HW, Speck SH.** 1999. B cells regulate murine gammaherpesvirus 68 latency. J Virol **73:**4651–4661.
22. **van den Berg A, Kroesen B-J, Kooistra K, de Jong D, Briggs J, Blokzijl T, Jacobs S, Kluiver J, Diepstra A, Maggio E, Poppema S.** 2003. High expression of B-cell receptor inducible gene *BIC* in all subtypes of Hodgkin lymphoma. Genes Chromosomes Cancer **37:**20–28. http://dx.doi.org/10.1002/gcc.10186.
23. **Haasch D, Chen Y-W, Reilly RM, Chiou XG, Koterski S, Smith ML, Kroeger P, McWeeny K, Halbert DN, Mollison KW, Djuric SW, Trevillyan JM.** 2002. T cell activation induces a noncoding RNA transcript sensitive to inhibition by immunosuppressant drugs and encoded by the proto-oncogene, *BIC*. Cell Immunol **217:**78–86. http://dx.doi.org/10.1016/S0008-8749(02)00506-3.
24. **Eis PS, Tam W, Sun L, Chadburn A, Li Z, Gomez MF, Lund E, Dahlberg JE.** 2005. Accumulation of miR-155 and BIC RNA in human B cell lymphomas. Proc Natl Acad Sci U S A **102:**3627–3632. http://dx.doi.org/10.1073/pnas.0500613102.
25. **Yin Q, Wang X, McBride J, Fewell C, Flemington E.** 2008. B-cell receptor activation induces BIC/miR-155 expression through a conserved AP-1 element. J Biol Chem **283:**2654–2662. http://dx.doi.org/10.1074/jbc.M708218200.
26. **Thai T-H, Calado DP, Casola S, Ansel KM, Xiao C, Xue Y, Murphy A, Frendewey D, Valenzuela D, Kutok JL, Schmidt-Supprian M, Rajewsky N, Yancopoulos G, Rao A, Rajewsky K.** 2007. Regulation of the germinal center response by microRNA-155. Science **316:**604–608. http://dx.doi.org/10.1126/science.1141229.
27. **Collins CM, Boss JM, Speck SH.** 2009. Identification of infected B-cell populations by using a recombinant murine gammaherpesvirus 68 expressing a fluorescent protein. J Virol **83:**6484–6493. http://dx.doi.org/10.1128/JVI.00297-09.
28. **Rodriguez A, Vigorito E, Clare S, Warren MV, Couttet P, Soond DR, van Dongen S, Grocock RJ, Das PP, Miska EA, Vetrie D, Okkenhaug K, Enright AJ, Dougan G, Turner M, Bradley A.** 2007. Requirement of *bic*/microRNA-155 for normal immune function. Science **316:**608–611. http://dx.doi.org/10.1126/science.1139253.
29. **Johnston RJ, Poholek AC, DiToro D, Yusuf I, Eto D, Barnett B, Dent AL, Craft J, Crotty S.** 2009. Bcl6 and Blimp-1 are reciprocal and antagonistic regulators of T follicular helper cell differentiation. Science **325:**1006–1010. http://dx.doi.org/10.1126/science.1175870.
30. **Baumjohann D, Preite S, Reboldi A, Ronchi F, Ansel KM, Lanzavecchia A, Sallusto F.** 2013. Persistent antigen and germinal center B cells sustain T follicular helper cell responses and phenotype. Immunity **38:**596–605. http://dx.doi.org/10.1016/j.immuni.2012.11.020.
31. **Collins CM, Speck SH.** 2014. Expansion of murine gammaherpesvirus latently infected B cells requires T follicular help. PLoS Pathog **10:**e1004106. http://dx.doi.org/10.1371/journal.ppat.1004106.
32. **Nurieva RI, Chung Y, Martinez GJ, Yang XO, Tanaka S, Matskevitch TD, Wang Y-H, Dong C.** 2009. Bcl6 mediates the development of T follicular helper cells. Science **325:**1001–1005. http://dx.doi.org/10.1126/science.1176676.
33. **Choi YS, Kageyama R, Eto D, Escobar TC, Johnston RJ, Monticelli L, Lao C, Crotty S.** 2011. ICOS receptor instructs T follicular helper cell versus effector cell differentiation via induction of the transcriptional repressor Bcl6. Immunity **34:**932–946. http://dx.doi.org/10.1016/j.immuni.2011.03.023.
34. **Grundhoff A, Sullivan CS, Ganem D.** 2006. A combined computational and microarray-based approach identifies novel microRNAs encoded by human gamma-herpesviruses. RNA **12:**733–750. http://dx.doi.org/10.1261/rna.2326106.
35. **Pfeffer S, Sewer A, Lagos-Quintana M, Sheridan R, Sander C, Grässer FA, van Dyk LF, Ho CK, Shuman S, Chien M, Russo JJ, Ju J, Randall G, Lindenbach BD, Rice CM, Simon V, Ho DD, Zavolan M, Tuschl T.** 2005. Identification of microRNAs of the herpesvirus family. Nat Methods **2:**269–276. http://dx.doi.org/10.1038/nmeth746.
36. **Gatto G, Rossi A, Rossi D, Kroening S, Bonatti S, Mallardo M.** 2008. Epstein-Barr virus latent membrane protein 1 trans-activates miR-155 transcription through the NF-κB pathway. Nucleic Acids Res **36:**6608–6619. http://dx.doi.org/10.1093/nar/gkn666.
37. **Feldman ER, Kara M, Coleman CB, Grau KR, Oko LM, Krueger BJ, Renne R, van Dyk LF, Tibbetts SA.** 2014. Virus-encoded microRNAs facilitate gammaherpesvirus latency and pathogenesis in vivo. mBio **5:**e00981–14. http://dx.doi.org/10.1128/mBio.00981-14.
38. **Vigorito E, Perks KL, Abreu-Goodger C, Bunting S, Xiang Z, Kohlhaas S, Das PP, Miska EA, Rodriguez A, Bradley A, Smith KGC, Rada C, Enright AJ, Toellner K-M, MacLennan ICM, Turner M.** 2007. microRNA-155 regulates the generation of immunoglobulin class-switched plasma cells. Immunity **27:**847–859. http://dx.doi.org/10.1016/j.immuni.2007.10.009.
39. **Hu R, Kagele DA, Huffaker TB, Runtsch MC, Alexander M, Liu J, Bake E, Su W, Williams MA, Rao DS, Möller T, Garden GA, Round JL, O'Connell RM.** 2014. miR-155 promotes T follicular helper cell accumulation during chronic, low-grade inflammation. Immunity **41:**605–619. http://dx.doi.org/10.1016/j.immuni.2014.09.015.
40. **Bossaller L, Burger J, Draeger R, Grimbacher B, Knoth R, Plebani A, Durandy A, Baumann U, Schlesier M, Welcher AA, Peter HH, Warnatz K.** 2006. ICOS deficiency is associated with a severe reduction of $CXCR5^+$ CD4 germinal center Th cells. J Immunol **177:**4927–4932. http://dx.doi.org/10.4049/jimmunol.177.7.4927.
41. **Warnatz K, Bossaller L, Salzer U, Skrabl-Baumgartner A, Schwinger W, van der Burg M, van Dongen JJ, Orlowska-Volk M, Knoth R, Durandy A, Draeger R, Schlesier M, Peter HH, Grimbacher B.** 2006. Human ICOS deficiency abrogates the germinal center reaction and provides a monogenic model for common variable immunodeficiency. Blood **107:**3045–3052. http://dx.doi.org/10.1182/blood-2005-07-2955.
42. **Cameron JE, Fewell C, Yin Q, McBride J, Wang X, Lin Z, Flemington EK.** 2008. Epstein-Barr virus growth/latency III program alters cellular microRNA expression. Virology **382:**257–266. http://dx.doi.org/10.1016/j.virol.2008.09.018.
43. **Lu F, Weidmer A, Liu C-G, Volinia S, Croce CM, Lieberman PM.** 2008. Epstein-Barr virus-induced miR-155 attenuates NF-κB signaling and stabilizes latent virus persistence. J Virol **82:**10436–10443. http://dx.doi.org/10.1128/JVI.00752-08.
44. **Barth S, Pfuhl T, Mamiani A, Ehses C, Roemer K, Kremmer E, Jäker C, Höck J, Meister G, Grässer FA.** 2008. Epstein-Barr virus-encoded

microRNA miR-BART2 down-regulates the viral DNA polymerase BALF5. Nucleic Acids Res **36:**666–675.
45. **Lu C-C, Li Z, Chu C-Y, Feng J, Feng J, Sun R, Rana TM.** 2010. MicroRNAs encoded by Kaposi's sarcoma-associated herpesvirus regulate viral life cycle. EMBO Rep **11:**784–790. http://dx.doi.org/10.1038/embor.2010.132.
46. **Ingle H, Kumar S, Raut AA, Mishra A, Kulkarni DD, Kameyama T, Takaoka A, Akira S, Kumar H.** 2015. The microRNA miR-485 targets host and influenza virus transcripts to regulate antiviral immunity and restrict viral replication. Sci Signal **8:**ra126. http://dx.doi.org/10.1126/scisignal.aab3183.
47. **Jiang S, Qi Y, He R, Huang Y, Liu Z, Ma Y, Guo X, Shao Y, Sun Z, Ruan Q.** 2015. Human cytomegalovirus microRNA miR-US25-1-5p inhibits viral replication by targeting multiple cellular genes during infection. Gene **570:**108–114. http://dx.doi.org/10.1016/j.gene.2015.06.009.
48. **Kluiver J, Haralambieva E, de Jong D, Blokzijl T, Jacobs S, Kroesen B-J, Poppema S, van den Berg A.** 2006. Lack of BIC and microRNA miR-155 expression in primary cases of Burkitt lymphoma. Genes Chromosomes Cancer **45:**147–153. http://dx.doi.org/10.1002/gcc.20273.
49. **Boss IW, Nadeau PE, Abbott JR, Yang Y, Mergia A, Renne R.** 2011. A Kaposi's sarcoma-associated herpesvirus-encoded ortholog of microRNA miR-155 induces human splenic B-cell expansion in NOD/LtSz-scid IL2Rγ$^{null}$ mice. J Virol **85:**9877–9886. http://dx.doi.org/10.1128/JVI.05558-11.
50. **Dahlke C, Maul K, Christalla T, Walz N, Schult P, Stocking C, Grundhoff A.** 2012. A microRNA encoded by Kaposi sarcoma-associated herpesvirus promotes B-cell expansion in vivo. PLoS One **7:**e49435. http://dx.doi.org/10.1371/journal.pone.0049435.
51. **Liu Y, Sun R, Lin X, Liang D, Deng Q, Lan K.** 2012. Kaposi's sarcoma-associated herpesvirus-encoded microRNA miR-K12-11 attenuates transforming growth factor beta signaling through suppression of SMAD5. J Virol **86:**1372–1381. http://dx.doi.org/10.1128/JVI.06245-11.
52. **Pratt ZL, Zhang J, Sugden B.** 2012. The latent membrane protein 1 (LMP1) oncogene of Epstein-Barr virus can simultaneously induce and inhibit apoptosis in B cells. J Virol **86:**4380–4393. http://dx.doi.org/10.1128/JVI.06966-11.
53. **Kim JH, Kim WS, Park C.** 2012. Epstein-Barr virus latent membrane protein-1 protects B-cell lymphoma from rituximab-induced apoptosis through miR-155-mediated Akt activation and up-regulation of Mcl-1. Leuk Lymphoma **53:**1586–1591. http://dx.doi.org/10.3109/10428194.2012.659736.
54. **Seto E, Moosmann A, Grömminger S, Walz N, Grundhoff A, Hammerschmidt W.** 2010. Micro RNAs of Epstein-Barr virus promote cell cycle progression and prevent apoptosis of primary human B cells. PLoS Pathog **6:**e1001063. http://dx.doi.org/10.1371/journal.ppat.1001063.
55. **Kim H, Choi H, Lee SK.** 2015. Epstein-Barr virus miR-BART20-5p regulates cell proliferation and apoptosis by targeting BAD. Cancer Lett **356:**733–742. http://dx.doi.org/10.1016/j.canlet.2014.10.023.
56. **Marquitz AR, Mathur A, Nam CS, Raab-Traub N.** 2011. The Epstein-Barr virus BART microRNAs target the pro-apoptotic protein Bim. Virology **412:**392–400. http://dx.doi.org/10.1016/j.virol.2011.01.028.
57. **Lei X, Bai Z, Ye F, Xie J, Kim C-G, Huang Y, Gao S-J.** 2010. Regulation of NF-κB inhibitor IκBα and viral replication by a KSHV microRNA. Nat Cell Biol **12:**193–199. http://dx.doi.org/10.1038/ncb2019.
58. **Liang D, Gao Y, Lin X, He Z, Zhao Q, Deng Q, Lan K.** 2011. A human herpesvirus miRNA attenuates interferon signaling and contributes to maintenance of viral latency by targeting IKKε. Cell Res **21:**793–806. http://dx.doi.org/10.1038/cr.2011.5.
59. **Qin Z, Kearney P, Plaisance K, Parsons CH.** 2010. Pivotal advance: Kaposi's sarcoma-associated herpesvirus (KSHV)-encoded microRNA specifically induce IL-6 and IL-10 secretion by macrophages and monocytes. J Leukoc Biol **87:**25–34. http://dx.doi.org/10.1189/jlb.0409251.
60. **Iizasa H, Wulff B-E, Alla NR, Maragkakis M, Megraw M, Hatzigeorgiou A, Iwakiri D, Takada K, Wiedmer A, Showe L, Lieberman P, Nishikura K.** 2010. Editing of Epstein-Barr virus-encoded BART6 microRNAs controls their Dicer targeting and consequently affects viral latency. J Biol Chem **285:**33358–33370. http://dx.doi.org/10.1074/jbc.M110.138362.
61. **Qiu J, Thorley-Lawson DA.** 2014. EBV microRNA BART 18-5p targets MAP3K2 to facilitate persistence in vivo by inhibiting viral replication in B cells. Proc Natl Acad Sci U S A **111:**11157–11162. http://dx.doi.org/10.1073/pnas.1406136111.
62. **Lin X, Liang D, He Z, Deng Q, Robertson ES, Lan K.** 2011. miR-K12-7-5p encoded by Kaposi's sarcoma-associated herpesvirus stabilizes the latent state by targeting viral ORF50/RTA. PLoS One **6:**e16224. http://dx.doi.org/10.1371/journal.pone.0016224.
63. **Bellare P, Ganem D.** 2009. Regulation of KSHV lytic switch protein expression by a virus-encoded microRNA: an evolutionary adaptation that fine-tunes lytic reactivation. Cell Host Microbe **6:**570–575. http://dx.doi.org/10.1016/j.chom.2009.11.008.
64. **Plaisance-Bonstaff K, Choi HS, Beals T, Krueger BJ, Boss IW, Gay LA, Haecker I, Hu J, Renne R.** 2014. KSHV miRNAs decrease expression of lytic genes in latently infected PEL and endothelial cells by targeting host transcription factors. Viruses **6:**4005–4023. http://dx.doi.org/10.3390/v6104005.
65. **Cramer EM, Shao Y, Wang Y, Yuan Y.** 2014. miR-190 is upregulated in Epstein-Barr virus type I latency and modulates cellular mRNAs involved in cell survival and viral reactivation. Virology **464–465:**184–195. http://dx.doi.org/10.1016/j.virol.2014.06.029.
66. **Yan Q, Li W, Tang Q, Yao S, Lv Z, Feng N, Ma X, Bai Z, Zeng Y, Qin D, Lu C.** 2013. Cellular microRNAs 498 and 320d regulate herpes simplex virus 1 induction of Kaposi's sarcoma-associated herpesvirus lytic replication by targeting RTA. PLoS One **8:**e55832. http://dx.doi.org/10.1371/journal.pone.0055832.
67. **Ellis-Connell AL, Iempridee T, Xu I, Mertz JE.** 2010. Cellular microRNAs 200b and 429 regulate the Epstein-Barr virus switch between latency and lytic replication. J Virol **84:**10329–10343. http://dx.doi.org/10.1128/JVI.00923-10.
68. **Lin Z, Wang X, Fewell C, Cameron J, Yin Q, Flemington EK.** 2010. Differential expression of the miR-200 family microRNAs in epithelial and B cells and regulation of Epstein-Barr virus reactivation by the miR-200 family member miR-429. J Virol **84:**7892–7897. http://dx.doi.org/10.1128/JVI.00379-10.
69. **Laichalk LL, Thorley-Lawson DA.** 2005. Terminal differentiation into plasma cells initiates the replicative cycle of Epstein-Barr virus in vivo. J Virol **79:**1296–1307. http://dx.doi.org/10.1128/JVI.79.2.1296-1307.2005.
70. **Siegel AM, Rangaswamy US, Napier RJ, Speck SH.** 2010. Blimp-1-dependent plasma cell differentiation is required for efficient maintenance of murine gammaherpesvirus latency and antiviral antibody responses. J Virol **84:**674–685. http://dx.doi.org/10.1128/JVI.01306-09.
71. **Wilson SJ, Tsao EH, Webb BLJ, Ye H, Dalton-Griffin L, Tsantoulas C, Gale CV, Du M-Q, Whitehouse A, Kellam P.** 2007. X box binding protein XBP-1s transactivates the Kaposi's sarcoma-associated herpesvirus (KSHV) ORF50 promoter, linking plasma cell differentiation to KSHV reactivation from latency. J Virol **81:**13578–13586. http://dx.doi.org/10.1128/JVI.01663-07.
72. **Bhende PM, Dickerson SJ, Sun X, Feng W-H, Kenney SC.** 2007. X-box-binding protein 1 activates lytic Epstein-Barr virus gene expression in combination with protein kinase D. J Virol **81:**7363–7370. http://dx.doi.org/10.1128/JVI.00154-07.
73. **Matar CG, Rangaswamy US, Wakeman BS, Iwakoshi N, Speck SH.** 2014. Murine gammaherpesvirus 68 reactivation from B cells requires IRF4 but not XBP-1. J Virol **88:**11600–11610. http://dx.doi.org/10.1128/JVI.01876-14.
74. **Lu D, Nakagawa R, Lazzaro S, Staudacher P, Abreu-Goodger C, Henley T, Boiani S, Leyland R, Galloway A, Andrews S, Butcher G, Nutt SL, Turner M, Vigorito E.** 2014. The miR-155–PU.1 axis acts on Pax5 to enable efficient terminal B cell differentiation. J Exp Med **211:**2183–2198. http://dx.doi.org/10.1084/jem.20140338.